

Next-to-leading order vs. quark off-shellness and intrinsic k_T in the Drell-Yan process *

O. Linnyk[†], S. Leupold, U. Mosel

Institut für Theoretische Physik, Universität Giessen, Germany
May 25, 2019

Abstract

We calculate the effects of next-to-leading order perturbative QCD as well as of the quark transverse motion and off-shellness on the Drell-Yan process cross section. By studying the $s \rightarrow \infty$ behaviour of the cross section in these approaches, we find that the effects of quark off-shellness and intrinsic- k_T parametrize those of higher twists. The transverse momentum of the Drell-Yan pairs and its evolution with the hard scale is also studied. Higher twist contributions to the dilepton p_T -spectrum are found to be large for presently accessible energies.

PACS numbers: 13.85.Qk, 12.38.Cy, 12.38.Qk

1 Introduction

At the future GSI-FAIR facility [1], several experiments will perform precise measurements of high mass lepton pair production in $\bar{p}p$ and $\bar{p}A$ collisions in order to determine parton distributions in the proton and in nuclei. Experiments GSI-PAX [2] and GSI-ASSIA [3] are going to study the polarized Drell-Yan process, while GSI-PANDA [4] will investigate unpolarized $\bar{p}p \rightarrow l^+l^-X$ and s as low as 15 GeV².

A good theoretical understanding of the Drell-Yan process at the level beyond the leading order (LO) and leading twist of perturbative QCD (pQCD) is necessary. Indeed, the effects beyond the LO pQCD are expected to be high at this low energy [5, 6]. These effects on the double differential cross section can be roughly parametrized by an overall K -factor, giving the discrepancy between the LO calculations and the data. However, in case of the triple differential cross section (*i.e.* transverse momentum distribution of dileptons), the corrections to LO pQCD cannot be parametrized by a constant factor, as we discuss below.

*work supported by BMBF

[†]olena.linnyk@theo.physik.uni-giessen.de

Applied to the Drell-Yan process $\bar{p}p \rightarrow l^+l^-X$, the leading order approximation of collinear pQCD predicts the correct dependence of the *double differential* Drell-Yan cross section $d^2\sigma/dM^2dx_F$ on the hard scale M . Here

$$x_F \equiv p_z/|p_z|_{max} \quad (1)$$

is the Feynman variable of the lepton pair and M its invariant mass. However, LO pQCD fails to reproduce

1. the magnitude of this cross section, the discrepancy being usually parametrized by a K -factor;
2. the average transverse momentum p_T of the dileptons;
3. the p_T -spectrum of Drell-Yan pairs, which is given by the *triple differential* cross section $d^3\sigma/dM^2dx_Fdp_T$.

Experimentally observed Drell-Yan lepton pairs have non-vanishing transverse momentum p_T , which can be as large as several GeV. However, in leading order of pQCD, the cross section is proportional to $\delta(p_T)$. Indeed, in collinear pQCD, both the transverse momentum and the light cone energy of quarks inside hadrons are neglected compared to the large component of the quark momentum, parallel to the hadron momentum. Thus, the initial state, *i.e.* the colliding quark and antiquark to be annihilated into a lepton pair, has no transverse momentum. Therefore, the final state has zero transverse momentum, too.

The diagrams contributing to the Drell-Yan process in addition to the LO parton model mechanism (a quark from one hadron annihilates with an antiquark from another hadron into a virtual photon) are divided into two classes: those of higher orders of α_S and those of higher twists. Calculating next-to-leading order contributions and refitting the parton distributions accordingly, one can reduce the discrepancy with the data on the double-differential Drell-Yan cross section [7, 8]. Moreover, the higher twists are vanishing in the limit of infinite energy. However, these power suppressed contributions can be large at realistic energies. We show in the present paper that the contribution of higher twists is essential for a proper description of the data on the triple-differential Drell-Yan cross section and propose a phenomenological model suitable to calculate these effects.

The lepton pairs can gain non-vanishing p_T due to two possible mechanisms

- processes of next-to-leading order (NLO) in α_S ,
- quark transverse motion and off-shellness.

In the former case, the dilepton pair recoils against an additional jet in the final state. Such processes exist at higher order in α_S . An example is given by the production of a gluon besides the virtual photon (see Fig. 1a)

$$\bar{q}q \rightarrow l^+l^-g. \quad (2)$$

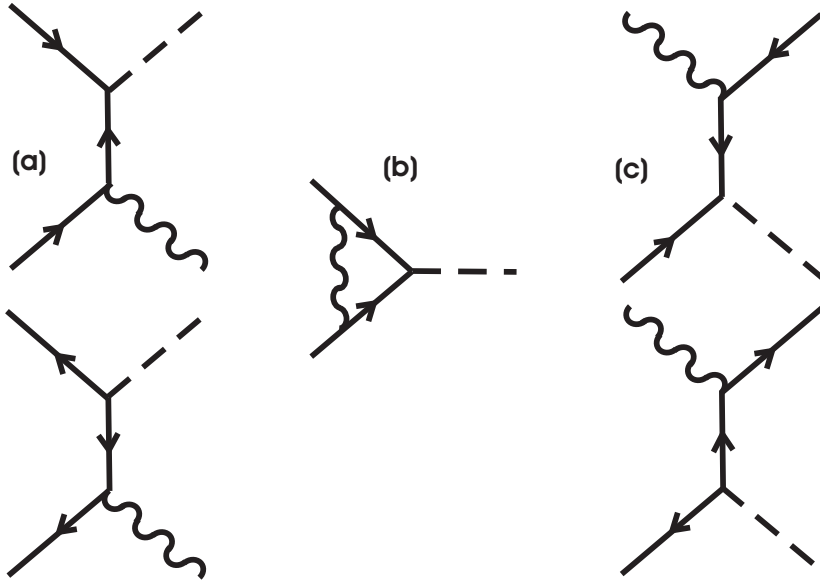


Figure 1: $O(\alpha_S)$ contributions to the Drell-Yan process: (a) gluon Bremsstrahlung, (b) vertex correction, (c) gluon Compton scattering. Virtual photons (dashed lines) split into lepton pairs, wavy lines denote gluons, arrows denote quarks. In each diagram, time runs from left to right.

Alternatively, final transverse momentum of the lepton pair can be caused by a non-vanishing transverse momentum of the initial state, *i.e.* by the non-collinearity of quarks inside the colliding hadrons. In this case, the recoil transverse momentum is carried by hadron remnants, formed by the “spectator” partons. In addition, the quark and gluon off-shellness can have a large effect for some observables, as has been recently shown in [9] and [10]. The parton off-shellness arises due to interaction between the partons in one hadron and constitutes a higher twist effect.

In the present paper, we study the Drell-Yan process cross section and the transverse momentum p_T of Drell-Yan pairs in both aforesaid approaches. In section 2, we calculate in collinear pQCD the mean $\langle p_T^2 \rangle_{pert}$, which is the part of the lepton p_T^2 generated by the next-to-leading order process (2). This method allows us to study the evolution of $\langle p_T^2 \rangle_{pert}$ with s and M . However, it turns out that the magnitude of the experimentally measured p_T cannot be described by NLO alone. On the other hand, the experimental data are reproduced much better by a model, taking into account both the intrinsic transverse momentum and the off-shellness of quarks in the proton, as will be shown in section 3. In this model there is no need for a K -factor. Instead, we describe both shape and magnitude of double as well as triple differential cross sections by extracting a quark-off-shellness from the data, which allows a physical interpretation. We expand the cross section in this model in powers of $1/s$ at $s \rightarrow \infty$ in order to relate the phenomenological result to higher twist corrections in section 4. We conclude in section 5.

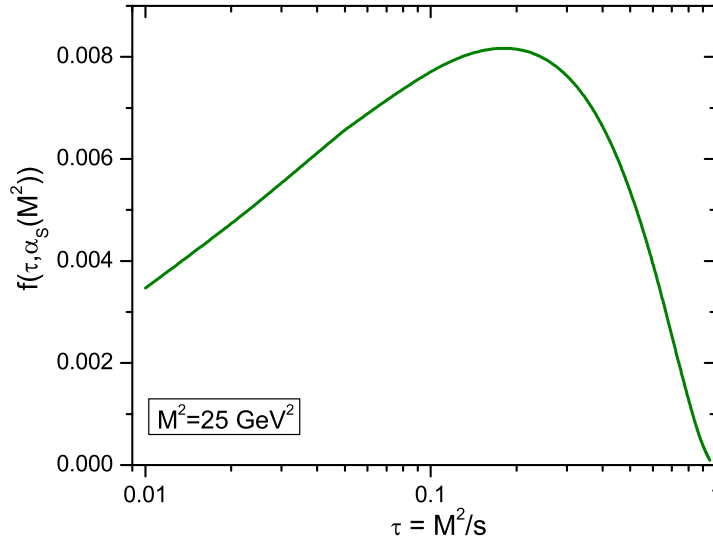


Figure 2: Function $f(\tau, \alpha_s)$ introduced in (6). This function governs the evolution of the p_T of Drell-Yan pairs with s and M^2 at NLO perturbative QCD.

2 Transverse momentum of Drell-Yan leptons in next-to-leading order of pQCD

First, let us consider the average p_T of the Drell-Yan pairs produced in $\bar{p}p$ collisions in the scope of conventional perturbative QCD. Consequently, intrinsic transverse momentum and off-shellness of the quarks are neglected for the duration of the current section. Therefore, important features are missing and we do not expect to reproduce the experimental p_T in this section.

At NLO of perturbative QCD, several diagrams contribute to the triple differential cross section, see Fig. 1. Among these, the vertex corrections do not generate transverse momentum. Therefore, we are interested in the gluon Bremsstrahlung and gluon Compton scattering. The pair with invariant mass M has a transverse momentum that relates to the scattering angle as [12]

$$p_T^2 = \frac{(\hat{s} - M^2)^2}{4\hat{s}} \sin^2 \Theta, \quad (3)$$

where $\hat{s} = x_1 x_2 s$ is the total squared energy of the colliding partons in terms of their momentum fractions in the collinear approximation, and Θ is the scattering angle of the outgoing lepton pair with respect to the incoming quark momentum in the quark centre of mass system.

In particular, the gluon Compton scattering contributes to the pairs with $p_T \gtrsim M$ [11], *i.e.* in the tail of the p_T distribution. On the other hand, the gluon Bremsstrahlung process generates the bulk of the Drell-Yan pairs with

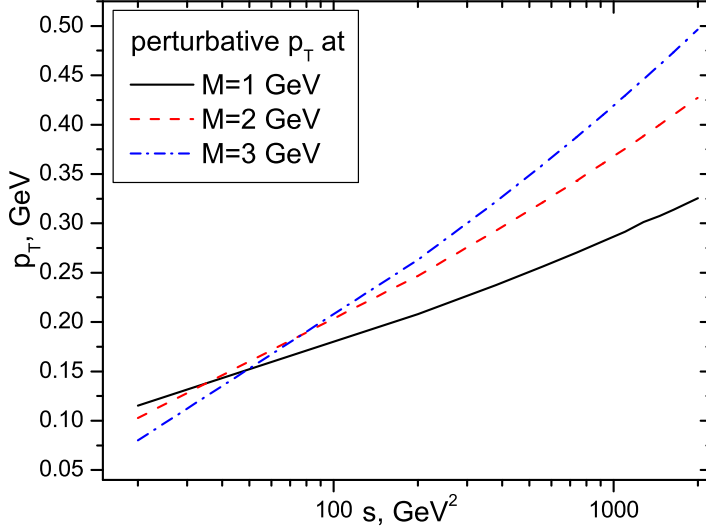


Figure 3: Evolution of the NLO perturbative component of Drell-Yan pair transverse momentum $p_T \equiv \sqrt{\langle \vec{p}_T^2 \rangle_{pert}}$ with s at different values of M .

a non-vanishing perturbatively generated p_T . According to [12], the cross section of the process $\bar{q}q \rightarrow g + \mu^+ \mu^-$ in NLO pQCD is given by

$$\frac{d^2 \hat{\sigma}}{dM^2 d \cos \Theta} = \frac{8\alpha^2 e_q^2 \alpha_S}{27M^2} \frac{\hat{s} - M^2}{\hat{s}^2 \sin^2 \Theta} \left\{ 1 + \cos^2 \Theta + 4 \frac{M^2 \hat{s}}{(\hat{s} - M^2)^2} \right\}. \quad (4)$$

By convoluting the sub-process cross section (4) with parton distributions, one expects to obtain the p_T distribution of the Drell-Yan pairs. Unfortunately, the resulting cross section is singular at $p_T = 0$ [13]; therefore the triple differential cross section cannot be described by NLO perturbative QCD. In order to be able to compare the NLO result with other approaches and with experiment, the authors of [12] and [14] proposed instead to calculate the average squared transverse momentum of Drell-Yan dileptons

$$\langle p_T^2 \rangle_{pert} = \frac{\int p_T^2 (d^2 \sigma_{NLO} / dp_T dM^2) dp_T}{d\sigma_{NLO} / dM^2}, \quad (5)$$

which is finite. In formula (5), $d\sigma_{NLO}$ is the double differential hadronic Drell-Yan cross section at the next-to-leading order.

The result is

$$\langle p_T^2 \rangle_{pert} = \alpha_S(M^2) s f(\tau, \alpha_S(M^2)), \quad (6)$$

where $\tau \equiv M^2/s$. Therefore, in the leading power of $\alpha_S(M^2)$, the mean squared p_T of Drell-Yan pairs is proportional to s , to α_S , and to a functional of parton distributions $f(\tau, \alpha_S)$ derived in [12]. Based on (6), it is sometimes concluded that $\langle \vec{p}_T^2 \rangle_{pert}$ scales linearly with s [15, 16, 17]. However, there is an

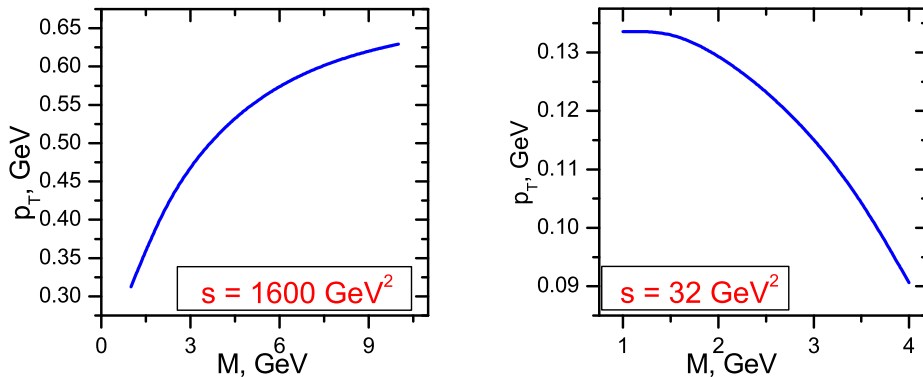


Figure 4: Perturbatively generated $p_T \equiv \sqrt{\langle \vec{p}_T^2 \rangle_{pert}}$ in NLO.

additional nonlinear dependence on s in $f(\tau, \alpha_S(M^2))$ through its dependence on $\tau \equiv M^2/s$. The dependence of f on α_S is introduced by the scaling violations in the parton distributions, while the dependence of f on τ arises from the gluon Bremsstrahlung cross section [12].

In order to determine the evolution of $\langle \vec{p}_T^2 \rangle_{pert}$ with M and \sqrt{s} , we have calculated the function $f(\tau, \alpha_S(M^2))$ numerically, using a recent parametrization [22] for parton distributions. The result is shown in Fig. 2. The position of the peak of f slightly shifts to the right with growing M . We see that only for a narrow region around $\tau \approx 0.2$, $f(\tau, \alpha_S)$ is approximately constant with τ and $\langle p_T^2 \rangle_{pert}$ is proportional to s .

The resulting dependence of $p_T \equiv \sqrt{\langle \vec{p}_T^2 \rangle_{pert}}$ on s and M is plotted in Fig. 3 and 4, respectively. One can see in Fig. 3 that the evolution of perturbative p_T with s is almost logarithmic, in contrast to the naïve expectation of being proportional to \sqrt{s} . Furthermore, the slope of the logarithmic rise with s depends on M . Note that there is an interesting cross-over at about $s \approx 50 \text{ GeV}^2$ (Fig. 3). While the perturbative $\langle p_T^2 \rangle_{pert}$ of Drell-Yan pairs increases with increasing M at high center of mass energy \sqrt{s} (see Fig. 4(a)), it decreases with M at low s (for instance, in Fig. 4(b) at $s = 32 \text{ GeV}^2$ relevant for the future PANDA experiment [4]) due to phase-space limitations.

3 Effects of non-collinearity and off-shellness of quarks in the proton

The transverse momentum distribution of Drell-Yan dileptons $d\sigma/dM^2 dx_f dp_T^2$ in the NLO perturbative QCD is singular at $p_T = 0$ [12, 16, 18] and underestimates experimental data at high p_T [19, 20]. Neither can the average p_T of Drell-Yan pairs be reproduced in NLO. Indeed, p_T calculated in the previous

section is around 0.6 GeV at $s = 1600 \text{ GeV}^2$ and $M \approx 7 \text{ GeV}$ (see Fig. 4(a)). This value is about a factor of 2 smaller than the width of the p_T distribution measured by the Fermilab experiment E866 [6]. We have to conclude that NLO pQCD is insufficient to describe present data on p_T of Drell-Yan pairs.

Natural approach to generate additional p_T is to take into account the primordial transverse momentum of quarks in the proton. The primordial quark transverse momentum is a non-perturbative effect and, from the uncertainty principle, averages at $\gtrsim 200 \text{ MeV}$. On the other hand, we will show that the higher twist effect of the intrinsic k_T on the Drell-Yan cross section is of the same order as the effect of non-vanishing quark off-shellness in proton, which is caused by the interaction of partons of one hadron in the initial state. Therefore, both the intrinsic k_T and quark off-shellness have to be taken into account for the sake of consistency.

The data on triple differential cross section also favor a model taking into account both non-collinearity and off-shellness of quarks. Such a model was proposed and tested against the E866 data [6] in earlier publications [5, 10]. The method utilizes phenomenological transverse momentum distribution and an off-shellness distribution (spectral function) of quarks in the proton.

This approach is based on the factorization assumption and on a second assumption that the soft part of the cross section can be approximated by a product of functions of the quark k^+ momentum, the transverse momentum, and the virtuality $m^2 \equiv k^+k^- - \vec{k}_T^2$. The part dependent on k^+ and k_T is

$$g_q(M^2, \xi, \vec{k}_T) = g(\vec{k}_T)q(\xi, M^2), \quad (7)$$

where $q(\xi, M^2)$ denotes parton distribution of quark flavor q at momentum fraction ξ . We use a Gaussian distribution of quark intrinsic transverse momentum k_T

$$g(\vec{k}_T) = \frac{1}{4\pi D^2} \exp\left(-\frac{\vec{k}_T^2}{4D^2}\right), \quad (8)$$

the mean squared partonic intrinsic transverse momentum being $\langle \vec{k}_T^2 \rangle = 4D^2$. The quark virtuality distribution also cannot be calculated from first principles. Using analogy to many body theory, we parametrize the quark virtuality distribution as a Breit-Wigner with width Γ

$$A(m) = \frac{1}{\pi} \frac{\Gamma}{m^2 + \frac{1}{4}\Gamma^2}. \quad (9)$$

The exact off-shell kinematics as well as the off-shell and non-collinear subprocess cross section (at LO in α_S) are used.

The cross section of the process '*hadron A* + '*hadron B*' $\rightarrow l^+l^+X$ in this approach is [10]

$$\begin{aligned} \frac{d^3\sigma}{dM^2 dx_F dp_T^2} &= \sum_q \int d\vec{k}_{1\perp} \int d\vec{k}_{2\perp} \int_0^\infty dm_1 \int_0^\infty dm_2 \int_0^1 d\xi_1 \int_0^1 d\xi_2 A(m_1)A(m_2) \\ &\times g_q^A(M^2, \xi_1, \vec{k}_{1\perp}) \bar{g}_q^B(M^2, \xi_2, \vec{k}_{2\perp}) \frac{d^3\hat{\sigma}_q(m_1, m_2, \vec{k}_{1\perp}, \vec{k}_{2\perp})}{dM^2 dx_F dp_T^2}, \quad (10) \end{aligned}$$

in which not only the three-dimensional (longitudinal and transverse) motion of partons, but also the virtualities of the active quark and anti-quark are explicitly taken into account by means of a phenomenological double-unintegrated parton density.

In (10), the following off-shell partonic cross section is used

$$\begin{aligned}
\frac{d\hat{\sigma}}{dM^2 dx_F dp_T^2} &= \kappa' \left[2M^4 - M^2 (m_1^2 - 6m_1 m_2 + m_2^2) - (m_1^2 - m_2^2)^2 \right] \\
&\times \delta \left(M^2 - m_1^2 - m_2^2 - \xi_1 \xi_2 P_1^- P_2^+ - \frac{(m_1^2 + \vec{k}_{1\perp}^2)(m_2^2 + \vec{k}_{2\perp}^2)}{\xi_1 \xi_2 P_1^- P_2^+} + 2\vec{k}_{1\perp} \vec{k}_{2\perp} \right) \\
&\times \delta \left(x_F - \frac{\sqrt{s}}{s - M^2} \left\{ \xi_2 P_2^+ - \xi_1 P_1^- + \frac{(m_1^2 + \vec{k}_{1\perp}^2)}{\xi_1 P_1^-} - \frac{(m_2^2 + \vec{k}_{2\perp}^2)}{\xi_2 P_2^+} \right\} \right) \\
&\times \delta \left((\vec{k}_{1\perp} + \vec{k}_{2\perp})^2 - p_T^2 \right), \tag{11}
\end{aligned}$$

with

$$\kappa' = \frac{2\alpha^2 e_q^2}{3M^4 N_c \sqrt{(k_1 \cdot k_2)^2 - m_1^2 m_2^2}}. \tag{12}$$

In (11),

$$\epsilon_1 \equiv \frac{1}{2} \left(\xi_1 P_1^- + \frac{(m_1^2 + \vec{k}_{1\perp}^2)}{\xi_1 P_1^-} \right), \quad \epsilon_2 \equiv \frac{1}{2} \left(\xi_2 P_2^+ + \frac{(m_2^2 + \vec{k}_{2\perp}^2)}{\xi_2 P_2^+} \right), \tag{13}$$

where

$$(P_1^\mp)^2 = (P_2^\pm)^2 = \frac{s}{2} - M_N^2 \pm \sqrt{\left(\frac{s}{2}\right)^2 - M_N^2 s} \tag{14}$$

in the hadron center of mass system¹.

In the scaling limit ($s \rightarrow \infty$, $s/M^2 = \text{const}$), the spectral functions effectively drop out due to normalization (*cf.* discussion later), and the hadronic cross section (10) goes to

$$\frac{d^3\sigma}{dM^2 dx_F dp_T^2} = \sum_q \Phi_q(x_1, x_2) \left(\frac{d^2\hat{\sigma}_q}{dM^2 dx_F} \right)_{LO} \frac{1}{8D^2} \exp\left(-\frac{p_T^2}{8D^2}\right), \tag{15}$$

where

$$\Phi_q(x_1, x_2) \equiv q^A(x_1) \bar{q}^B(x_2) + \bar{q}^A(x_1) q^B(x_2), \tag{16}$$

$$\left(\frac{d^2\hat{\sigma}_q}{dM^2 dx_F} \right)_{LO} = \frac{4\pi\alpha^2 e_q^2}{9M^4} \frac{x_1 x_2}{x_1 + x_2} (1 - x_1 x_2), \tag{17}$$

¹Formula (11) is the corrected version of the erroneous formula (39) in [10] rewritten in Lorentz invariant form. Numerically, the difference between the two expressions is less than 1% in the kinematics studied in [10] but might be large at $x_F \rightarrow 1$ and $p_T \gg M$.

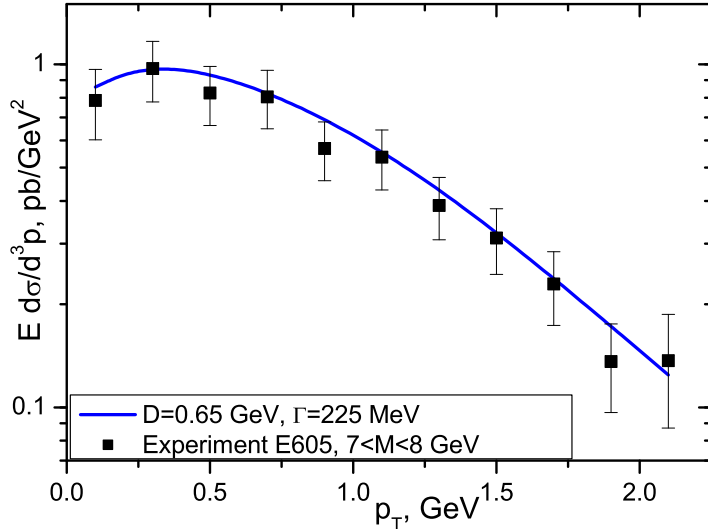


Figure 5: Prediction for the p_T spectrum of Drell-Yan dileptons in our model at $\sqrt{s} = 40$ and $x_F = 0.1$ as compared to the data of experiment E605 [23].

and the parton momentum fractions (x_1, x_2) are defined via

$$M^2 = x_1 x_2 s; \quad (18)$$

$$x_F = (x_2 - x_1)/(1 - x_1 x_2). \quad (19)$$

Note that the term $x_1 x_2$ in the denominator in (19) is sometimes omitted in textbooks, where an approximate definition $x_F \approx 2p_z/\sqrt{s}$ is used in stead of (1).

In [10], our model was compared to the data on the triple differential Drell-Yan cross section $d^3\sigma/dM^2 dx_F dp_T$ from experiment E866 [6] at Fermilab in pp collisions at 800 GeV incident energy. Both the slope and magnitude of the p_T distribution of the Drell-Yan pairs were described well without the need for a K -factor. In particular, the experimentally measured $\langle p_T^2 \rangle$ is reproduced in this model by fitting the model parameter D (the dispersion of the quark intrinsic transverse momentum). At $s = 1600 \text{ GeV}^2$, we obtained $D = 0.5 \pm 0.18 \text{ GeV}$. On the other hand, the detailed shape of the distribution turned out to be sensitive to the off-shellness, giving $\Gamma = 50 - 300 \text{ MeV}$ (depending on the mass bin) for this particular experiment.

The distribution of the transverse momentum of lepton pairs produced in the Drell-Yan process off *nuclei* $pA \rightarrow l^+ l^- X$ also can be reproduced within this model. For example, in Fig. 5 the calculation for the transverse momentum spectrum of Drell-Yan dileptons of our model is compared to the data of the experiment E605 [23] on $p \text{ Cu}$ collisions at $\sqrt{s} = 38.8 \text{ GeV}$,

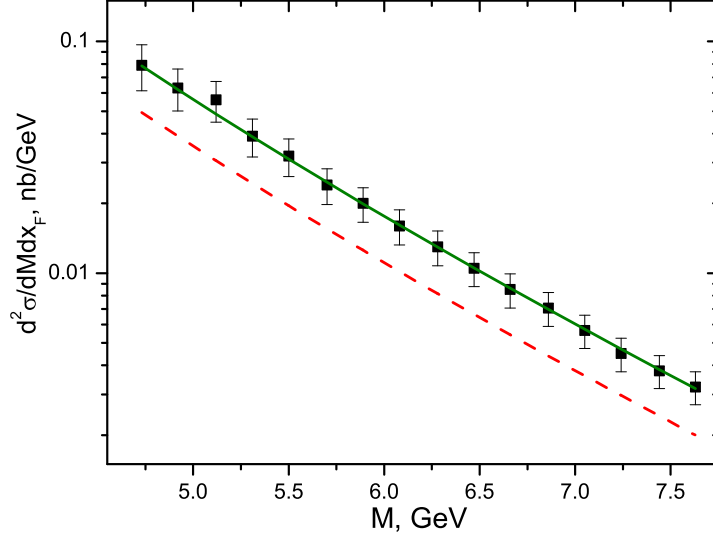


Figure 6: Result of LO collinear QCD for a double differential Drell-Yan cross section (dashed line) at $\sqrt{s} = 20$ and $x_F = 0.1$ as compared to experiment E439 [21]. Solid line is the LO result scaled up with a factor $K = 1.6$.

$x_F = 0.1$. The cross section plotted in Fig. 5 is

$$E \frac{d^3\sigma}{d^3p} \equiv \frac{2E}{\pi\sqrt{s}} \frac{d\sigma}{dx_F dp_T^2} = \frac{2E}{\pi\sqrt{s}} \int_{\text{bin}} \frac{d\sigma}{dM^2 dx_F dp_T^2} dM^2. \quad (20)$$

where

$$E \equiv \sqrt{M^2 + p_T^2 + x_F^2(s - M^2)^2/(4s)}. \quad (21)$$

The model parameters D , Γ used in the calculations were fitted to data on $pp \rightarrow l^+l^-X$ in [10] and no readjustment was done for the pA case.

In the present paper, we want to make a consistent comparison with NLO results. However, the triple differential cross section $E d^3\sigma/d^3p$ is singular for $p_T \rightarrow 0$ in every fixed order of pQCD [8, 13]. We, therefore, apply the described model now to the double differential cross section $d^2\sigma/dM dx_F$. The K -factor, which is needed to increase the magnitude of the LO prediction for the double differential Drell-Yan process cross section so that it agrees with the data, can be decreased from 2 to 1.1 by taking into account NLO processes [7]. In order to determine, what part of this LO K -factor can be accounted for by the model with intrinsic k_T and off-shellness of quarks, we compare data to the triple differential cross section (10) integrated over p_T .

In Fig. 6, the Drell-Yan process cross section $d^2\sigma/dM dx_F$ predicted at leading order of perturbative QCD (dashed line) is compared to the data of the Fermilab experiment E439 [21] on pW collision at 400 GeV incident energy, at $x_F = 0.1$. The LO prediction lies below the data. The solid line

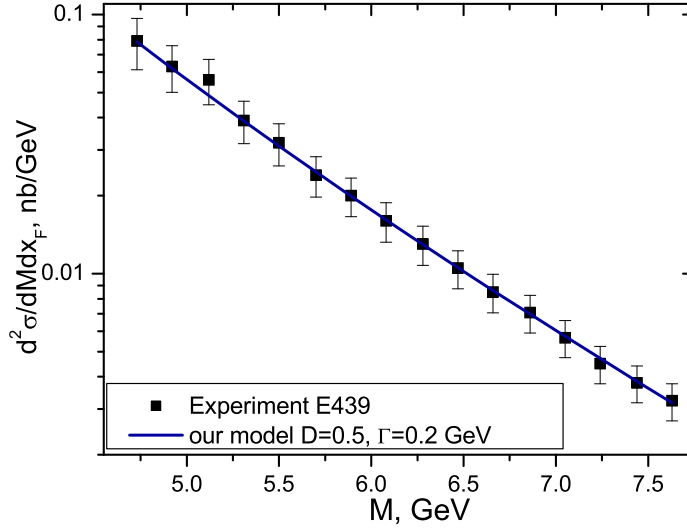


Figure 7: Drell-Yan cross section in our model at $D = 500$ MeV, $\Gamma = 200$ MeV compared to the data of experiment E439 [21]. $K = 1$.

shows the LO curve scaled up with a factor $K = 1.6$. The K -factor depends somewhat on the parametrization of parton distributions used. We use here the parametrization [22]. If one assumes a larger contribution of sea quarks, the K -factor needed to describe the data is lower.

In order to calculate the double differential Drell-Yan process cross section in our model, we first find the triple differential cross section from (10). The double differential cross section is obtained using

$$\frac{d^2\sigma}{dM^2 dx_F} \equiv \int_0^{(p_T^2)_{max}} \frac{d^3\sigma}{dM^2 dx_F dp_T^2} dp_T^2. \quad (22)$$

Note that the maximum transverse momentum of the Drell-Yan pair $(p_T^2)_{max}$ is fixed by kinematics

$$(p_T^2)_{max} = \frac{(s + M^2 - M_R^2)^2}{4s} - x_F^2 \frac{(s - M^2)^2}{4s} - M^2, \quad (23)$$

where M_R^2 is the minimal invariant mass of the undetected remnant.

The data are reproduced well (see Fig. 7) with $K = 1$. We conclude that in the experimentally relevant region the K -factor of the double differential Drell-Yan cross section can be explained by two alternative scenarios: either as an effect of higher orders of perturbative QCD as shown in [7, 8] or as an effect of non-collinearity and off-shellness of quarks in our phenomenological approach. The experimental cross section magnitude can be reproduced in

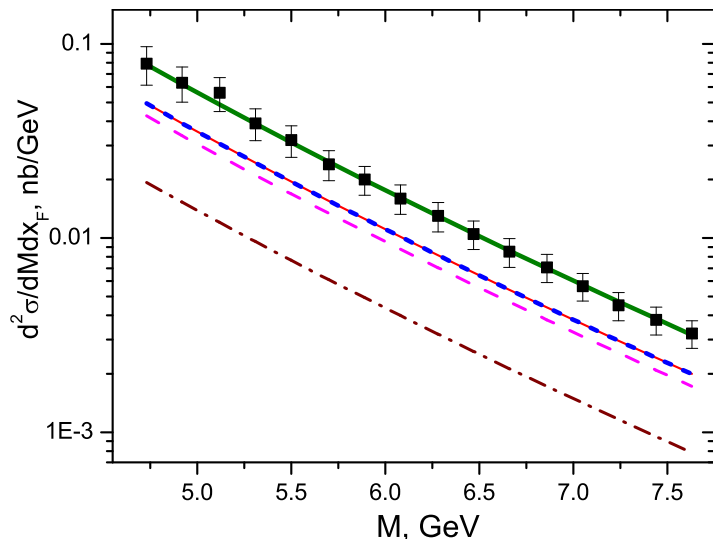


Figure 8: Drell-Yan cross section in a simplified intrinsic- k_T approach at $D = 50$ MeV (short dash), $D = 250$ MeV (dash), $D = 500$ MeV (dash-dot) compared to LO pQCD (thin solid line) and the data of experiment E439 [21]. The solid line gives the theoretical curves multiplied by D -dependent K -factors fitted to the data. Everywhere, $\Gamma = 0$.

NLO calculations by fitting the renormalization scale or in our model by fitting the parameters D and Γ . The latter explanation of the K -factor has the advantage that it can explain also the triple differential cross section.

In the following, we additionally study the relative importance of quark off-shellness and quark intrinsic transverse motion by comparing our result to that of the intrinsic- k_T approach. The intrinsic- k_T approach [24] is a limiting case of our model at $\Gamma \rightarrow 0$. The factorization assumption in this case gives

$$\frac{d^4\sigma}{dM^2 dx_F d\vec{p}_T} = g(\vec{k}_{T1}) \otimes g(\vec{k}_{T2}) \otimes \frac{d^2\hat{\sigma}(\vec{k}_{T1}, \vec{k}_{T2})}{dM^2 dx_F} \delta(\vec{p}_T - \vec{k}_{T1} - \vec{k}_{T2}). \quad (24)$$

The formula is often simplified by neglecting the dependence of $\hat{\sigma}$ on \vec{k}_{T1} and \vec{k}_{T2} , for example in [15] and in PYTHIA [25]. In this case, the p_T spectrum of Drell-Yan pairs $d^3\sigma/dM^2 dx_F dp_T^2$ is also simply a Gaussian in p_T^2 . The cross section (24) has to be integrated over the azimuthal angle of the lepton pair and over p_T^2 according to (22). Because of the finite integration interval in (22), we do not recover the normalization of the k_T -distribution (8), but obtain a suppression that increases with D .

The double differential Drell-Yan process cross section in the intrinsic k_T approach with collinear sub-process cross section at three values of D is compared to the LO of pQCD and the data of the experiment E439 in Fig. 8. The magnitude of the measured cross section cannot be reproduced in this simplified intrinsic k_T approach, in which the dependence of the partonic $d\hat{\sigma}$

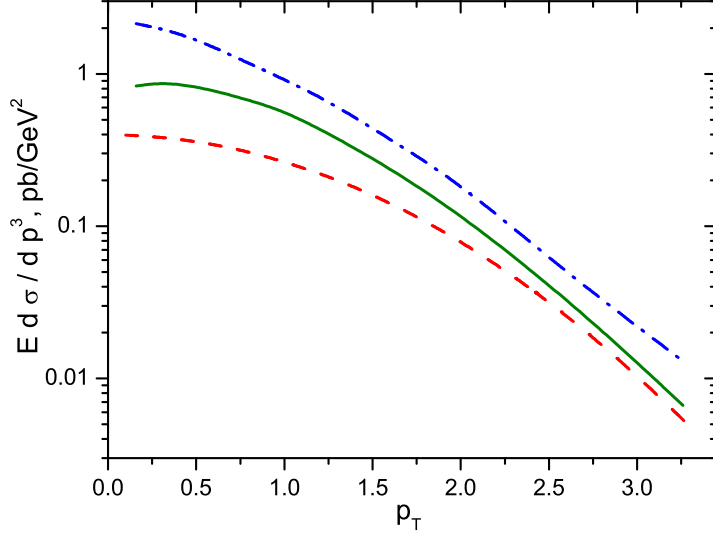


Figure 9: Drell-Yan cross section in three approaches: simplified intrinsic- k_T with collinear sub-process cross section (dash), full intrinsic- k_T (dash-dot), our model at $\Gamma = 225$ MeV (solid). Everywhere, $D = 550$ MeV, $\sqrt{s} = 40$ GeV, $M \approx 7.5$ GeV.

on \vec{k}_{1T} and \vec{k}_{2T} are neglected. Just as in LO of pQCD, scaling with an overall K -factor ranging from 1.6 to 4 is necessary to describe the data. It is apparent from Fig. 8 that the K -factor extracted from the data is D -dependent. Therefore, this scaling factor should be understood as a phenomenological parameter and not as a measure of higher order corrections.

Summarizing, there are three phenomenological approaches to the Drell-Yan process beyond LO pQCD:

1. our model, accounting for both intrinsic transverse momentum ($D \neq 0$) and off-shellness ($\Gamma \neq 0$) of quarks;
2. intrinsic- k_T approach ($D \neq 0$), which is the limiting case of our model at $\Gamma = 0$;
3. simplified intrinsic- k_T approach ($\Gamma = 0$), in which the primordial transverse momentum is not zero ($D \neq 0$), but the non-collinearity of the $\bar{q}q \rightarrow l^+l^-$ sub-process cross section $d\hat{\sigma}$, *i.e.* its dependence on \vec{k}_1 and \vec{k}_2 , is neglected.

We compare the effects of primordial k_T , non-collinearity of $d\hat{\sigma}$ and quark off-shellness by plotting the triple differential Drell-Yan cross section calculated in the three aforesaid phenomenological approaches in Fig. 9. The simplified intrinsic- k_T approach gives a Gaussian for the p_T -distribution (dash line). As we will show in the next section, the approximation of $\Gamma = 0$ and collinear $d\hat{\sigma}$

is equivalent to restricting oneself to the leading term in the twist expansion, that is, in the case of the unpolarized Drell-Yan process, the expansion in powers of $1/M$. In Fig. 9, the importance of higher twist corrections in the Drell-Yan process is illustrated by the difference between the solid and dash lines.

The part of higher-twist effects incorporated in the full intrinsic- k_T approach changes the distribution considerably (*cf.* the dash and dash-dot curves in Fig. 9). On the other hand, additional higher twist effects, modelled by quark off-shellness and given by the difference between the dash-dot and solid curves, are of the same order. We conclude that higher twists in the Drell-Yan process can be large and that we have to take into account both non-collinearity and off-shellness of quarks in order to model them.

4 Twist nature of the phenomenological corrections

In the previous section we have shown that the double differential Drell-Yan cross section is reproduced by a model accounting for intrinsic k_T and off-shellness of quarks without a need for a K -factor. In addition, the p_T distribution of the Drell-Yan pairs can be explained in our model [10], but not in NLO of pQCD [19, 20]. Therefore, the effects of quark off-shellness and intrinsic k_T do not arise solely from the diagrams of NLO pQCD. Instead, we will show that they parametrize higher twist processes. Some of the diagrams that contribute to the Drell-Yan cross section at higher twist are shown in Fig. 10. Gluon radiation in the initial state and gluon exchange between the active parton and spectators generate intrinsic k_T and virtuality of quarks in the proton in the Drell-Yan process. Some of these processes (for example, the gluon exchanges that connect factorized regions - the hard sub-process and a soft matrix element) are suppressed by powers of s in the scaling limit. However, the power-suppressed corrections give a sizable contribution to the transverse momentum spectrum of Drell-Yan pairs at finite s accessible in modern experiments.

In this section, we investigate the relationship of NLO and higher twist corrections to those calculated in our phenomenological approach by comparing their behaviour in the Drell-Yan scaling limit, in which $s \rightarrow \infty$ and $M^2 \rightarrow \infty$ with $\tau = s/M^2$ finite. The NLO corrections are proportional to α_s ; therefore we expect a logarithmic dependence of these corrections on the hard scale $s \sim M^2$. On the other hand, higher twist contributions are suppressed in powers of s in the scaling limit.

In order to determine whether the effects of quark virtuality and intrinsic k_T are leading twist, we study the behaviour of the Drell-Yan cross section calculated in our model in the scaling limit. For comparison, note that the

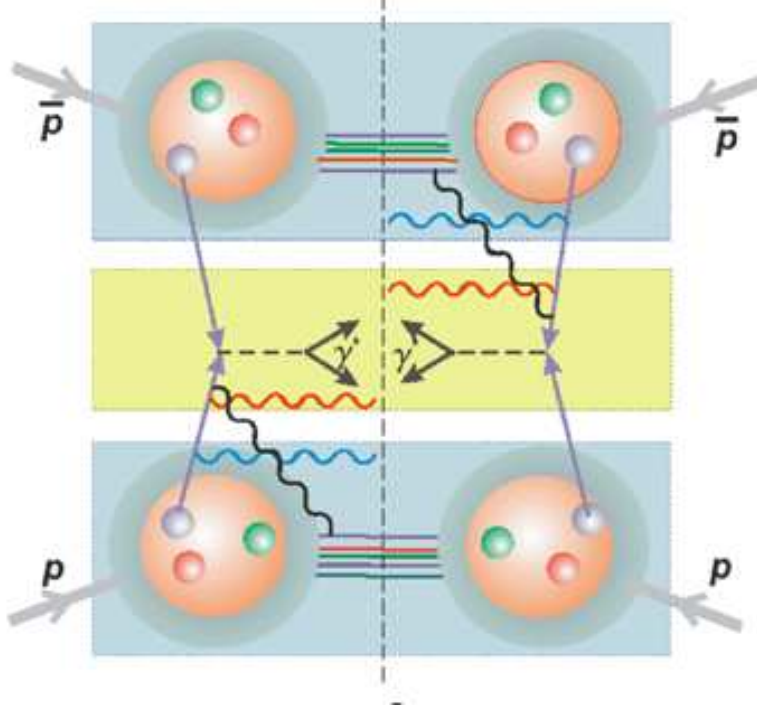


Figure 10: Example of gluon radiation diagrams generating intrinsic k_T and virtuality of quarks in the proton as probed in the Drell-Yan process.

lowest order triple differential cross section is given by

$$\left(\frac{d^3\sigma}{dM^2 dx_F dp_T^2} \right)_{LO} = \sum_q \Phi_q(x_1, x_2) \left(\frac{d^2\hat{\sigma}_q}{dM^2 dx_F} \right)_{LO} \delta(p_T^2). \quad (25)$$

From (15) one observes that the corrections to the p_T distribution of the Drell-Yan pairs due to quark non-collinearity in the proton are not suppressed in the limit $s \rightarrow \infty$. The model taking into account the intrinsic k_T of partons therefore parametrizes some of the leading twist effects. This part of the model effects, i.e. the Gaussian smearing of p_T , is related to contributions of the higher order diagrams of the perturbative QCD series as is shown for deep inelastic scattering at small Bjorken x in [8].

On the other hand, the corrections to the LO cross section generated by the k_T dependence of the sub-process cross section $d\hat{\sigma}$ are suppressed by powers of the hard scale s . Therefore, they represent part of the higher twist effects. To study this in more detail, we expand the cross section (10) in a series in $1/s$ around $s = \infty$, keeping this time not only the leading term, as it has been done in (15), but all the terms that are suppressed by less than s^2 . We analyze the cross section at the specific value of $x_F = 0$ to make the formulas less bulky.

We start from the general formula (10). First, we expand the integrand of (10) in $1/s$. For this purpose not only $d\hat{\sigma}$ of (11) has to be evaluated at

$s \rightarrow \infty$, but also the combination of parton distributions (7) that enters (10) has to be Taylor expanded around ($\xi_1 = \sqrt{\tau}, \xi_2 = \sqrt{\tau}$). The arguments of parton distributions ξ_1 and ξ_2 are fixed after integrating out the δ -functions in (11). As a result, the probed parton light cone momentum fractions depend on quark intrinsic transverse momentum and off-shellness. After integrating (10) over ξ_1, ξ_2 and angles, the quantity $\Phi_q(\tilde{\xi}_1, \tilde{\xi}_2)$ enters the hadronic cross section formula. Here, $\tilde{\xi}_1$ and $\tilde{\xi}_2$ are

$$\tilde{\xi}_1 = \sqrt{\tau} \left(1 + \frac{p_T^2/2 - m_2^2 - k_2^2}{\sqrt{\tau}s} + O\left(\frac{1}{s^2}\right) \right), \quad (26)$$

$$\tilde{\xi}_2 = \sqrt{\tau} \left(1 + \frac{p_T^2/2 - m_1^2 - k_1^2}{\sqrt{\tau}s} + O\left(\frac{1}{s^2}\right) \right). \quad (27)$$

Keeping the first two orders in the Taylor expansion of $\Phi_q(\tilde{\xi}_1, \tilde{\xi}_2)$ and in the $1/(\tau s)$ -expansion of $d\hat{\sigma}$, we obtain:

$$\begin{aligned} \frac{d\sigma_q^3}{dM^2 dx_F dp_T^2} \Big|_{x_F=0} &= \frac{\alpha^2 e_q^2 (1-\tau)}{8\pi D^4 12\tau^2 s^3} \int_0^\infty dk_2^2 \int_{(k_1^2)_{min}}^{(k_1^2)_{max}} dk_1^2 \int_0^{(m_2)_{max}} dm_2 \int_0^{(m_1)_{max}} dm_1 \\ &\times \frac{A(m_1)A(m_2) \exp\left(-\frac{k_1^2+k_2^2}{4D^2}\right)}{\sqrt{k_1^2 k_2^2 - \frac{1}{4}(p_T^2 - k_1^2 - k_2^2)^2}} \left[G_1^q(\tau) \frac{\sqrt{\tau}}{8} \left(\frac{p_T^2}{2} - m_1^2 - k_1^2 \right) \right. \\ &+ G_2^q(\tau) \frac{\sqrt{\tau}}{8} \left(\frac{p_T^2}{2} - m_2^2 - k_2^2 \right) \\ &\left. + T^q(\tau) \left(\frac{\tau s}{8} + \frac{p_T^2}{6} + \frac{k_1^2}{6} + F(m_1, m_2) \right) + O\left(\frac{1}{s}\right) \right], \quad (28) \end{aligned}$$

where

$$(k_1^2)_{min} \equiv (p_T - k_2)^2; \quad (29)$$

$$(k_1^2)_{max} \equiv (p_T + k_2)^2; \quad (30)$$

$$(m_1)_{max} \equiv \sqrt{\tau s + p_T^2/2 - k_1^2}; \quad (31)$$

$$(m_2)_{max} \equiv \sqrt{\tau s + p_T^2/2 - k_2^2}; \quad (32)$$

$$\begin{aligned} F(m_1, m_2) &\equiv \frac{1}{\tau} \left(2(m_1^2 + m_2^2)(\tau/8 + x_1^2/6 - x_1\sqrt{\tau}/6) + (m_1 + m_2)^2\tau/6 \right. \\ &+ m_1^2\tau/6 + (m_1^2 - m_2^2)x_1\sqrt{\tau}/6 - m_1^2\tau\sqrt{\tau}/(6x_1) \\ &\left. + \frac{\tau}{8}(m_1^2 - m_2^2 + k_1^2 - k_2^2) \right); \quad (33) \end{aligned}$$

$$T^q(\tau) \equiv \Phi^q(\sqrt{\tau}, \sqrt{\tau}); \quad (34)$$

and

$$G_1^q(\tau) \equiv \frac{\partial \Phi^q(x_1, x_2)}{\partial x_1} \Big|_{(x_1=\sqrt{\tau}, x_2=\sqrt{\tau})}, \quad (35)$$

$$G_2^q(\tau) \equiv \frac{\partial \Phi^q(x_1, x_2)}{\partial x_2} \Big|_{(x_1=\sqrt{\tau}, x_2=\sqrt{\tau})} \quad (36)$$

are the derivatives of the parton distribution product around $(\sqrt{\tau}, \sqrt{\tau})$.

To further investigate the dependence of the integral (28) on s , we have to specify the quark spectral function. Indeed, the integration variables m_1 and m_2 at $s \rightarrow \infty$ can be arbitrarily big, as can be seen from (31) and (32). Therefore, only after the integration over m_i has been performed can we judge whether any off-shellness generated term is sub-leading in s and how much it is suppressed. On the other hand, the integration over m_i provides additional terms $\sim k^2/s$, making the separation of off-shellness and intrinsic k_T effects involved.

In the following, we perform the analytical integration of (28), assuming different functional forms for the quark off-shellness distribution $A(m)$:

1. a Dirac delta-function $\delta(m)$,
2. a Breit-Wigner function (Lorentz distribution) with a constant parameter Γ , see (9).

In the former case, the model reduces to the intrinsic- k_T approach. Integrations over m_i drop out, while the remaining integrals over k_1^2 and k_2^2 can be done analytically via Bessel functions. As the result, one finds the leading term (15) plus $1/(\tau s)$ suppressed contributions.

Let us now consider the second, more general, case. The cross section for $A(m) = \delta(m)$ is the limiting case of the formulas given below for a Breit-Wigner distribution (9) at $\Gamma = 0$. Inserting the distribution (9) into (28), performing all the integrations and keeping only the first few leading terms in $1/M$, we obtain (note that $M^2 = \tau s \rightarrow \infty$, as $s \rightarrow \infty$)

$$\begin{aligned} \left. \frac{d^3\sigma_q}{dM^2 dx_F dp_T^2} \right|_{x_F=0} &= \frac{1}{8D^2} \exp\left(-\frac{\bar{p}_T^2}{8D^2}\right) \sum_q \left(\frac{d^2\hat{\sigma}_q}{dM^2 dx_F} \right)_{LO} [T^q(\tau) \\ &\quad + \{4T^q(\tau) - \sqrt{\tau}(G_1^q(\tau) + G_2^q(\tau))\} \frac{1}{\pi} \frac{\Gamma}{M} \\ &\quad + \left\{ \sqrt{\tau}(G_1^q(\tau) + G_2^q(\tau)) \left(\frac{p_T^2}{4} - 2D^2 \right) + \frac{8}{3} T^q(\tau) \left(\frac{5p_T^2}{4} + D^2 \right) \right\} \frac{1}{M^2} \\ &\quad + O\left(\frac{\Gamma}{M^3}\right)]. \quad (37) \end{aligned}$$

At leading twist, the Gaussian distribution of p_T (15) is recovered. However, it is modified by the higher twists, suppressed in the limit $s \rightarrow \infty$, but substantial at finite s accessible in experiment. The term proportional to $1/M = 1/\sqrt{\tau s}$ is p_T -independent and leads to an overall enhancement of the cross section, while the p_T -dependent terms proportional to $1/M^2$ additionally modify the shape of the p_T distribution.

The contribution of the off-shellness of quarks to (37) is given by the summands proportional to Γ . It is suppressed by powers of M and vanishes in the intrinsic k_T approach, in which $\Gamma = 0$. Thus, the model, which additionally accounts for quark off-shellness, parametrizes more higher twist effects than the intrinsic- k_T approach alone.

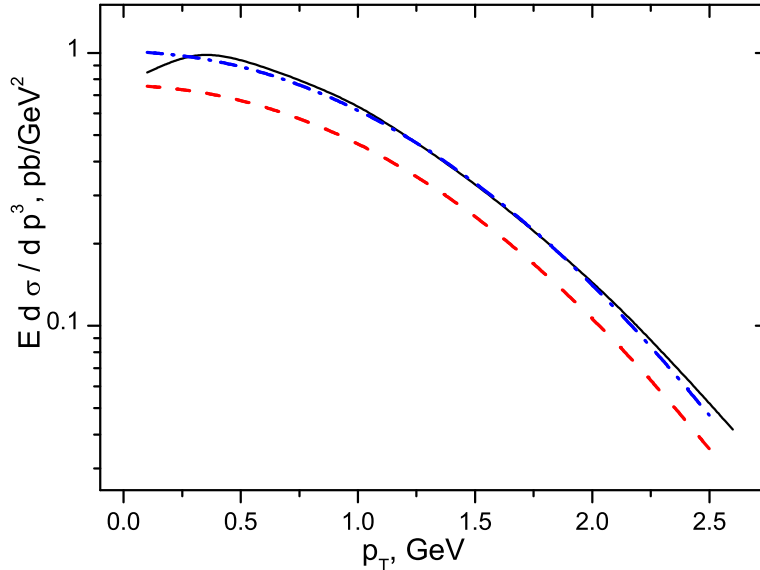


Figure 11: Cross section of $pp \rightarrow l^+l^-X$ at $M \approx 7$ GeV, $s = 1600$ GeV² in our model (solid), in the leading order in $1/M^2$ (dash), up to the next-to-leading order in $1/M^2$ expansion (dash-dot). $D = 650$ MeV, $\Gamma = 225$ MeV, $x_F = 0$.

It is interesting that the effects due to the finite quark width Γ appear in the expansion at odd powers of $1/M$ in contrast to those due to the intrinsic- k_T . The first Γ -dependent correction is proportional to $1/M = 1/\sqrt{\tau s}$. Therefore, the corrections due to the virtuality of quarks seem to have a non-analytical dependence on s as $(\tau s)^{-1/2}$. In order to preserve analyticity of the cross section we have to assume that the quark width Γ has a particular scaling behavior at large hard scale of the probe $M = \sqrt{\tau s}$:

$$\Gamma(M) \sim \frac{1}{M}, \text{ as } M \rightarrow \infty. \quad (38)$$

Then, in (37), the terms proportional to Γ/M and the terms proportional to $1/M^2$ together constitute the dominant higher twist correction to the leading result (15) in the scaling limit.

We expect the formula (37) to give a good approximation to the Drell-Yan cross section (10) at large finite M and s . In order to illustrate this, we compare the result of the exact calculations, i.e. the numerical integration of (10), to the leading twist approximation (15) and to the next-to-leading twist result (37) in two regimes:

- at $M \approx 7$ GeV and $s = 1600$ GeV², see Fig. 11;
- at $M = 1$ GeV and $s = 30.25$ GeV² relevant for FAIR [1], see Fig. 12.

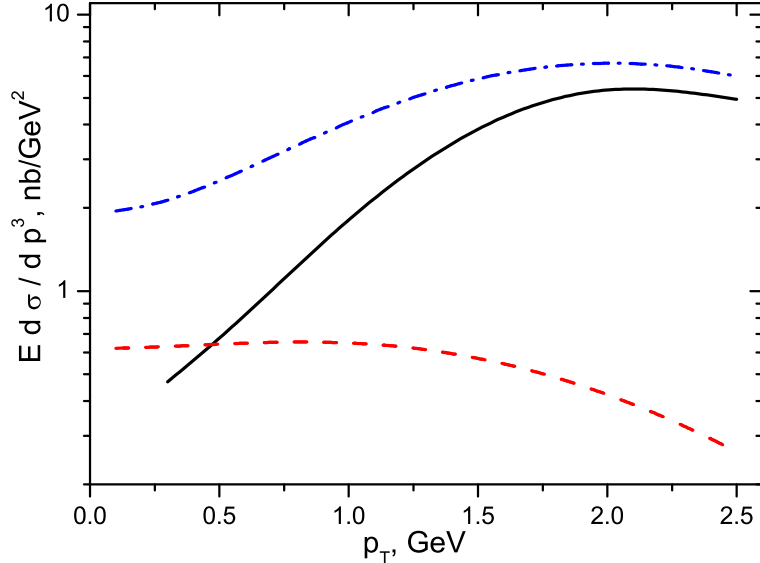


Figure 12: Cross section of $p\bar{p} \rightarrow l^+l^-X$ at $M = 1$ GeV and $s = 30.25$ GeV² in our model (solid), in the leading order in $1/M^2$ (dash), up to the next-to-leading order in $1/M^2$ expansion (dash-dot). $D = 600$ MeV, $\Gamma = 250$ MeV, $x_F = 0$.

As expected, the sum of leading and next-to-leading terms of the power series (37) reproduces the full calculations quite well at M as high as 7 GeV. The approximate cross section has the same average magnitude and slope. Therefore, it is dominating the K -factor type corrections to the leading twist cross section. Only the bend of the cross section at low p_T , which is seen in the full calculations and in the data (Fig. 5), is not reproduced at the next-to-leading twist.

From the Fig. 12, one sees that our model predicts the higher twist effects to be very large at low M and s . The discrepancy between approximate and exact Drell-Yan cross sections is large in this regime, too, especially at low p_T . We conclude that one needs to go beyond the next-to-leading twist at this low M and s . In this region, our model becomes indispensable, because it effectively sums higher twists.

5 Conclusions

We have analyzed the double differential Drell-Yan cross section $d^2\sigma/dM^2dx_F$ and the p_T distribution of the Drell-Yan dileptons $d^3\sigma/dM^2dx_Fdp_T^2$ in two alternative approaches: collinear perturbative QCD at next-to-leading order and a model, which makes use of phenomenological distributions for k_T and off-shellness of quarks in the proton.

We find that the transverse momentum spectrum of the Drell-Yan pairs

at the next-to-leading order pQCD disagrees with experiment both quantitatively and qualitatively. In contrast, we find that the phenomenological model with off-shell non-collinear partons successfully describes both the double differential Drell-Yan cross section and the p_T spectrum of Drell-Yan pairs without the need of a K factor.

The analysis of the Drell-Yan process cross section in our model in the Drell-Yan scaling limit has shown that the phenomenological model parametrizes higher twist effects. Higher twist contributions, being suppressed by powers of the hard scale, are usually considered to be small. As a rule, they are neglected in pQCD calculations. However, as we have shown, the power suppressed effect can be large at realistic energies.

We have found that the intrinsic transverse momentum of quarks generates both leading twist and $1/(\tau s) = 1/M^2$ suppressed effects. This is in line with our analysis of section 1, which has shown that only part of observed $\langle p_T^2 \rangle$ can be explained in NLO pQCD. In addition, we have shown that next-to-leading twist corrections due to quark off-shellness change the overall cross section magnitude and are, therefore, responsible for a part of the K-factor type discrepancy between the leading order pQCD and data.

If a Breit-Wigner parametrization for the quark off-shellness distribution is used, the next-to-leading contribution is proportional to $\Gamma/\sqrt{\tau s}$. This leads us to suggest that the quark width Γ scales as $\Gamma(M) \sim 1/M$ at large hard scale $M = \sqrt{\tau s}$.

The formula that we obtained for the Drell-Yan cross section at the next-to-leading twist level can be very useful for applications, for example, in an event generator. Indeed, it requires no numerical integration, while providing a good approximation to the full calculations at $M \gtrsim 5$ GeV. However, at $M \lesssim 5$ GeV, one has to go beyond the next-to-leading order in the power series and use the formulas of [10].

The results show that the higher twist corrections to high energy processes can be large. Therefore, a detailed study and modelling of these effects is necessary, if one hopes to reliably extract quark and gluon properties from hadron scattering data.

References

- [1] K. Peters, AIP Conf. Proc. **796**, 355 (2005).
- [2] P. Lenisa [PAX Collaboration], AIP Conf. Proc. **792**, 1023 (2005).
- [3] V. Abazov *et al.* [ASSIA Collaboration], arXiv:hep-ex/0507077.
- [4] M. Kotulla *et al.*, Technical Progress Report for PANDA, (2005), http://www.ep1.rub.de/~panda/db/papersdb/pc19-050217_panda_tpr.pdf
- [5] O. Linnyk, S. Leupold and U. Mosel, Phys. Rev. D **73**, 037502 (2006), arXiv:hep-ph/0506134.

- [6] J. C. Webb, PhD thesis, New Mexico State University (2003), arXiv:hep-ex/0301031.
- [7] W. J. Stirling M. R. Whalley, J.Phys.G:Nucl.Part.Phys. **19**, D1 (1993).
- [8] R. K. Ellis, W. J. Stirling and B. R. Webber, “QCD and collider physics,” Cambridge University Press (1996).
- [9] J. Collins and H. Jung, arXiv:hep-ph/0508280.
- [10] O. Linnyk, S. Leupold and U. Mosel, Phys. Rev. D **71**, 034009 (2005), arXiv:hep-ph/0412138.
- [11] E. L. Berger, L. E. Gordon and M. Klasen, Phys. Rev. D **58**, 74012 (1998).
- [12] G. Altarelli, G. Parisi and R. Petronzio, Phys. Lett. B **76**, 351 (1978).
- [13] J. Raufeisen, PhD thesis, Heidelberg University (2000), arXiv:hep-ph/0009358.
- [14] H. Fritzsche and P. Minkowski, Phys. Lett. B **73**, 80 (1978).
- [15] U. D’Alesio and F. Murgia, Phys. Rev. D **70**, 074009 (2004), arXiv:hep-ph/0408092.
- [16] E. Leader and E. Predazzi, Camb. Monogr. Part. Phys. Nucl. Phys. Cosmol. **4** 1 (1996).
- [17] G. Altarelli, in “Geneva 1979, Proceedings of international conference on high energy physics, Vol.2,” 727 (1979).
- [18] F. Halzen and D. M. Scott, Phys. Rev. Lett. **40**, 1117 (1978).
- [19] K. Kajantie and R. Raitio, Nucl. Phys. **B139**, 72 (1978).
- [20] I. R. Kenyon, Rept. Prog. Phys. **45**, 1261 (1982).
- [21] S. R. Smith *et al.*, Phys. Rev. Lett. **46**, 1607 (1981).
- [22] M. Glück, E. Reya, and A. Vogt, Eur. Phys. J. C **5**, 461 (1998), arXiv:hep-ph/9806404.
- [23] G. Moreno *et al.*, Phys. Rev. D **43**, 2815 (1991).
- [24] M. Fontannaz and D. Schiff, Nucl. Phys. B **132**, 457 (1978); C.-Y. Wong and H. Wang, Phys. Rev. C **58**, 376 (1998), arXiv:nucl-th/9802378; X.-N. Wang, Phys. Rev. C **61**, 064910 (2000), arXiv:nucl-th/9812021; Y. Zhang, G. Fai, G. Papp, G. Barnafoldi, and P. Levai, Phys. Rev. C **65**, 034903 (2002), arXiv:hep-ph/0109233.
- [25] T. Sjöstrand *et al.*, Comput. Phys. Commun. **135**, 238 (2001) arXiv:hep-ph/0010017.